Developmental changes in spinal neuronal properties, motor network configuration, and neuromodulation at free-swimming stages of Xenopus tadpoles

Citation for published version:
Currie, SP & Sillar, KT 2018, 'Developmental changes in spinal neuronal properties, motor network configuration, and neuromodulation at free-swimming stages of Xenopus tadpoles', *Journal of Neurophysiology*, vol. 119, no. 3, pp. 786-795. https://doi.org/10.1152/jn.00219.2017

Digital Object Identifier (DOI):
10.1152/jn.00219.2017

Developmental changes in spinal neuronal properties, motor network configuration and neuromodulation at free-swimming stages of *Xenopus* frog tadpoles.

Stephen P. Currie and Keith T. Sillar

School of Psychology and Neuroscience, University of St Andrews, St Marys Quad, St Andrews KY16 9JP, Scotland, UK.

Running Head: Development of tadpole spinal locomotor network

Corresponding author:

Keith T. Sillar

University of St Andrews,

School of Psychology and Neuroscience,

St Andrews, Fife KY169JP,

Scotland, United Kingdom

Email: kts1@st-andrews.ac.uk

Telephone: +44 1334 462050

Keywords

Author contributions:

KTS and SPC designed the experiments. SPC performed all experiments and data analysis. KTS and SPC drafted the manuscript.

ABSTRACT

We describe a novel preparation of the isolated brainstem and spinal cord from pro-metamorphic tadpole stages of the South African clawed frog (*Xenopus laevis*) that permits whole cell patch-clamp recordings from neurons in the ventral spinal cord. Previous research on earlier stages of the same species has provided one of the most detailed understandings of the design and operation of a CPG circuit. Here we have addressed how development sculpts complexity from this more basic circuit. The preparation generates bouts of fictive swimming activity either spontaneously or in response to electrical stimulation of the optic tectum, allowing an investigation into how the neuronal properties, activity patterns and neuromodulation of locomotor rhythm generation change during development. We describe an increased repertoire of cellular responses compared to younger larval stages and investigate the cellular level effects of nitrergic neuromodulation as well as the development of a sodium pump-mediated ultra-slow afterhyperpolarisation (usAHP) in these free-swimming larval animals.

Keywords: development, locomotion, nitric oxide, neuromodulation, *Xenopus*

NEW & NOTEWORTHY A novel *in vitro* brainstem/spinal cord preparation is described that enables whole cell patch-clamp recordings from spinal neurons in pro-metamorphic *Xenopus* tadpoles. Compared to the well-characterised earlier stages of development, spinal neurons display a wider range of firing properties during swimming and have developed novel cellular properties. This preparation now makes it feasible to investigate in detail spinal CPG maturation during the dramatic switch between undulatory and limb-based locomotion strategies during amphibian metamorphosis.

INTRODUCTION

The hatching stage tadpole of the frog, *Xenopus laevis*, (stage 37/38) has one of the most completely described motor control systems of any vertebrate. This has largely been due to the development of a preparation enabling patch-clamp recordings from pairs of synaptically coupled spinal neurons, which has allowed the spinal network for locomotion to be understood in cellular and synaptic detail (Roberts et al. 2010). Furthermore, research on the early larval stages - just a day or so later in development, but still before continuous free swimming begins - has provided several insights into how neural networks are modified to enable complex behaviour to emerge as ontogeny progresses (Sillar et al. 1991, 1992, Zhang et al. 2009, 2011). Here we describe a novel preparation that forms the foundation for the next steps in the study of motor control in *Xenopus* by enabling whole cell patch-clamp recordings from *in vitro* brainstem/spinal cords isolated from free-swimming pro-metamorphic (stages 50–58 Nieuwkoop and Faber 1956) tadpoles. At these stages, the tadpoles swim almost continuously, sculling with the caudal portion of their tail in order to retain a head-down hover, facilitating their lifestyle as obligate filter feeders (Hoff and Wassersug, 1986). At earlier stages of *Xenopus* development, swimming occurs in prolonged bouts following sensory stimulation and all neurons within the spinal network fire rhythmically throughout the swim cycle to maintain the coordinated muscle contraction underlying forward propulsion (Roberts et al. 2010). The aim of this study was to explore changes in the properties and modulation of spinal neurons that might account for the development of more flexible swimming behaviour and the switch from a primarily sessile existence to one where swimming occurs almost constantly (Currie et al. 2016). For instance, an important intrinsic property recently described in spinal neurons from earlier stages is the activity-dependent ultra-slow afterhyperpolarisation (usAHP; Zhang and Sillar 2012; Zhang et al. 2015), which results from increased activation of the sodium pump. The usAHP is thought to act as a form of internal memory for previous cellular activity. At early stages of development, the usAHP is detectable in about 50% of spinal locomotor neurons but whether this is a transient feature during early development or one that persists later in development is not known. Moreover, the effects of nitric oxide (NO), which is known to potently modulate fictive locomotion at these later stages (Currie et al. 2016), have not been investigated at the cellular level. Since the effects of endogenous NO at these stages are location-specific, complex and different from earlier stages, having switched from an inhibitory to an excitatory influence (Currie et al. 2016), NO's direct effect on spinal neurons is an important next step in understanding the role of nitrergic neuromodulation in this developing system.

METHODS

Animals and husbandry.

Experiments were performed on free-swimming, pro-metamorphic stages (50–58) of the South African clawed frog, *Xenopus laevis* (Nieuwkoop and Faber 1956). Animals were obtained by human chorionic gonadotrophin hormone-assisted (1,000 U/ml; Sigma) matings of adults selected from an in-house breeding colony. Fertilized ova were collected and reared in enamel trays until the first free-feeding stages, before being transferred to standard glass aquarium tanks. All procedures complied with the UK Animals (Scientific Procedures) Act 1986 and the European Community Council directive of 24 November 1986 (86/609/EEC) and were approved by the University of St. Andrews Animal Welfare Ethics Committee.

Dissection for whole cell recording.

In order to make single cell patch-clamp recordings in the ventral spinal cord of pro-metamorphic *Xenopus* tadpoles, the dissection employed during extracellular experiments (Combes et al. 2004; Currie et al. 2016) was modified. Briefly, after removal and destruction of the brain under MS222 anaesthesia, the remaining nervous system was cut free from the rest of the body. The caudal extent of the spinal cord was cut to completely isolate the brainstem and spinal cord and this tissue was then pinned down securely with sharpened tungsten wire pins in a recording chamber with a rotatable Sylgard platform. Using a finely etched tungsten needle, the spinal cord was then opened along the medio-lateral midline as far as the neurocoel from approximately the 12^{th} -15^{th} post-otic ventral root. At the caudal extent of this first cut, a second cut was made perpendicularly, approximately as deep as the dorso-ventral midline of the spinal cord, and all the way to the lateral extent of the cord. The free end of the spinal cord was then carefully peeled back towards the rostral end of the animal, removing most or all of the dorsal horn. Once at the level of the 12^{th} post-otic ventral root the dorsal portion of spinal cord was cut away using microscissors (see Fig. 1B). This modified preparation gave direct access to the ventral spinal cord, where the spinal circuits involved in motor control are presumed to lie. Moreover, exposing the ventral cord between the 12^{th} and 15^{th} ventral roots gave access to neurons assumed to be primarily involved in axial swimming patterns since they are located caudal to the ventral roots innervating the developing hindlimbs.

Electrophysiology.

The dissection and subsequent electrophysiological recordings were performed in 'HEPES' saline (composition in mM: 115 NaCl, 3 KCl, 2 CaCl2, 2.4 NaHCO3, 1 MgCl2, 10 Hepes, adjusted with 4 M NaOH to pH 7.4). Whole-cell patch-clamp recordings in current clamp mode were made using microelectrodes pulled on a Sutter P97 pipette puller from borosilicate glass capillaries (Harvard Apparatus Ltd.). All recordings were made from neurons at relatively ventral locations in the spinal cord, between the 11^{th} and 16^{th} post-otic ventral root. Patch pipettes were filled with 0.1% neurobiotin in the intracellular solution (composition in mM: 100 K-gluconate, 2MgCl2, 10 EGTA, 10 Hepes, 3 Na2ATP, 0.5 NaGTP adjusted to pH 7.3 with KOH) and had resistances of approximately 8MΩ. Extracellular ventral root recordings were made ipsilaterally to the exposed area for patch recording and generally caudally between the 16^{th} and 19^{th} post-otic ventral roots. Recordings in whole-cell mode were amplified with an Axoclamp 2B (Axon Instruments) amplifier and digitized using a CED power1401. All signals were displayed and saved on a PC using Spike2 software and all subsequent analysis performed in Dataview software (v 8.62, courtesy of W. J. Heitler, School of Biology, University of St Andrews, St Andrews, UK).

Neuron labelling.

Neurobiotin (0.1%) in the intracellular solution was used to label neurons for anatomical identification. Following electrophysiological recordings, the brainstem-spinal cord tissue was fixed in 2% glutaraldehyde in 0.1 M phosphate buffer (pH 7.2) overnight in the refrigerator (4°C). After they were rinsed with 0.1 M PBS (120 mM NaCl in 0.1 M phosphate buffer, pH 7.2), the animals were (1) washed in two changes of 1% Triton X-100 in PBS for 15 min with agitation, (2) incubated in a 1:300 dilution of extravidin peroxidase conjugate (Sigma Aldrich, UK) in PBS containing 0.5% Triton X-100 for 2–3 hr with agitation, (3) washed again in at least four changes of PBS, (4) presoaked in 0.08% diaminobenzidine in PBS (DAB solution) for 5 min, (5) moved to a second container with 0.075% hydrogen peroxide in DAB solution for 5 min, and (6) washed in running tap water. The nervous system was then dehydrated, cleared in methyl benzoate and xylene, and mounted whole, between two coverslips using Depex. Neuronal anatomy was observed using a Zeiss Axio Imager Ax10 at x20 and x40 magnification and measurements were made using Zen Imaging Pro (v10; Zeiss) software.

Pharmacological manipulations.

Saline during electrophysiological experiments was gravity fed from one of two stock chambers. This allowed switching between control and drug conditions via a three-way tap. Saline flowed to waste and was not recirculated. Drugs used were the NO donors S-nitroso-N-acetylpenicillamine (SNAP – 200μM) and Diethylamine NONOate (DEA-NO – 50 – 200μM). No obvious differences in drug effect were seen over this concentration range of DEA-NO (c.f. Currie et al, 2016). Drugs were dissolved in distilled H2O (18MΩ), aliquoted and then frozen, before being made up to final concentration in standard HEPES saline - the dilution of saline with H2O vehicle was <0.5%.

Statistical analysis.

Mean data was analysed using either a paired t-test; repeated measures ANOVA with Bonferroni correction; or in the case of normalised data, a Wilcoxon signed rank test and significance reported at either < 0.01 or < 0.05. Error bars represent the standard deviation of the mean. For the cumulative probability plots of PSP frequency and amplitude, the Kolmogorov-Smirnov test (K-S test) was employed at a significance level of 0.05. The bin sizes were standardised throughout at 0.1Hz for PSP frequency and 0.05mV for PSP amplitude. Statistical analyses were performed in SPSS (version 21; IBM), graphs were produced from custom written MATLAB scripts (The MathWorks, Inc.) and figures arranged in Adobe Illustrator CC (Adobe Systems, Inc.).

RESULTS

A major aim of this study was to explore developmental changes in neuronal, circuit and neuromodulation properties that accompany the transition to more flexible and continuous tadpole swimming behaviour compared to embryonic and early larval stage. In order to do this we have developed a new preparation that allows for whole cell patch-clamp recordings of neurons within the spinal cord at free-swimming pro-metamorphic stages (50-58; Nieuwkoop and Faber 1956) of *Xenopus* tadpoles (Fig. 1A,B). At these stages of development, bouts of fictive swimming readily occur spontaneously in *in vitro* preparations of the spinal cord and brainstem (Combes et al. 2004; see Fig. 1Ci), but similar bouts can also be evoked by brief electrical stimulation of the optic tectum (Fig. 1Cii). In both cases, the activity of individual rhythmically active neurons can be recorded and assessed simultaneously using this new preparation.

Neuronal activity during swimming

The data reported in this study derive from 104 neurons (9 identified anatomically as motorneurons (MNs) - see below) recorded in 83 preparations. During spontaneous episodes of swimming, rhythmically active spinal neurons generally fired action potentials in phase with the bursts of activity recorded from ipsilateral spinal ventral roots (Fig. 1C; 50/83 (60.2%) neurons where activity in a ventral root was present for comparison). In a typical neuron, the onset of ventral root activity coincided with or was just preceded by a depolarisation of the membrane potential, which then oscillated in phase with the rhythmic network activity recorded in the ventral root. Preceding the onset of rhythmic activity, 12/83 (14.5%) neurons initially fired tonically and the ventral root recording displayed a corresponding period of tonic discharge (see Fig. 1Ci). As the ventral root began to burst rhythmically these cells also switched into a rhythmic pattern of firing, with volleys of action potentials interspersed with periods of subthreshold activity (Fig. 1Ci middle inset; Cii, inset). Over the course of an episode, the activity often waxed and waned and the neuron was often de-recruited but continued to receive rhythmic synaptic drive in time with the ventral root bursts (see inset in Fig. 1Cii). Rhythmic activity was often followed by tonic ventral root discharge and neuronal firing (Fig. 1Ci) or faded away gradually with sporadic spiking activity (Fig.1Cii). While the majority of recorded neurons fired transiently and only during periods of network activity, a subset (7/104; 6.7%) discharged tonically at rest (Fig. 2). However, these neurons were also apparently linked to locomotor output since during network activity their firing was often altered. The changes in firing pattern could be quite subtle, as in the modulation of tonic firing frequency seen in figure 2A, or they could be more dramatic, switching in and out of a rhythmic firing pattern phase-related to the locomotor cycle, as in figure 2B.

Basic firing properties

The average resting membrane potential of all recorded neurons was -57.8 +/- 6.67mV (n = 104 from N = 83 animals). From rest, the injection of a short (2ms) current pulse was capable of eliciting an action potential with a mean threshold for activation of 487.34 +/- 390.89pA. All but one recorded neuron (see Fig. 3Ci) was capable of firing repetitively during current injection and fired at higher frequency as the amplitude of the current pulse was increased (Fig. 3A). The frequency-current plots in Fig. 3Aiii illustrate representative examples of both a lower threshold (open black circles; also see Fig. 3Ai) and a higher threshold neuron (filled black circles; also see Fig. 3Aii). Both of these neurons were later identified as MNs (see below for details).

A novel property found in a small proportion of unidentified neurons in pro-metamorphic tadpoles, was an apparently intrinsic rhythmogenic capacity (Fig. 3Bi). Thus in 2/104 neurons (2%), depolarising current injection resulted in an oscillation of the membrane potential, with superimposed bursts of action potentials interspersed with periods where the membrane potential was re-polarised below spike threshold. The intrinsic membrane oscillation was relatively slow, in the range of 0.5-1Hz, in comparison to the membrane oscillation associated with swimming, which are typically 4-6Hz. The firing pattern was similar to the intrinsic bursting seen in low threshold zebrafish MNs that are recruited during the slowest swimming speeds (Gabriel et al. 2011; Menelaou and McLean 2012), but in *Xenopus* this has never been documented in publications based on many thousands of recordings at the embryonic and early larval stages of tadpole development. The neurons had relatively low rheobases of 110pA and 310pA, respectively, and both fired rhythmically during swimming (Fig. 3Bii).

As at early larval stage 42 (Sillar et al. 1991), neurons fired variably during episodes of fictive swimming and could fire multiple spikes during each motor burst (see inset in Fig. 1Cii). The exception to this was a single neuron that had a relatively depolarised resting membrane potential of -50mV and during swimming fired one broad action potential per cycle (Fig. 3Ci-ii – for comparison Fig 3Cii also shows the MN from Fig. 3Aii). Moreover, injection of supra-threshold current was unable to elicit repetitive firing, even at 400% of the rheobase (Fig. 3Ciii). This neuron therefore displayed physiological characteristics reminiscent of an embryonic descending interneuron (dIN; Li et al. 2006; see discussion).

Recording from motorneurons

Following patch clamp recordings, neurobiotin originating from within the patch solution allowed post-hoc analysis of the anatomy of a subset of individual spinal neurons (see e.g. Fig. 4). Definitive anatomical identification of spinal neurons was not possible in the majority of cases due in part to the quality of the fills, but also due to the lack of conformity of successful stainings with the well-characterised spinal neurons from earlier in *Xenopus* development. Nevertheless, 9/101 (8.9%) filled neurons were confirmed as MNs based on their axonal projections that exited the spinal cord via a ventral root (Fig. 4Ai & iii). The MNs had a medially located soma and generally had dendrites that projected laterally into the marginal zone (Fig. 4Aiv). The primary axon exited the soma and initially ran close to the midline of the spinal cord (Fig. 4Aiv). The axon projected ipsilaterally and caudally over several spinal segments (Fig. 4Ai-iii) before turning and exiting via a ventral root (Fig. 4Ai & iii). All identified MNs projected caudally from the soma and exited via a ventral root between 4 and 9 spinal segments away (mean = 6.33 +/- 1.58 segments). Occasionally physiological characterisation of MNs was also possible (Fig. 4B). In 3/104 recorded neurons, including 1 in addition to the 9 anatomically identified MNs, each action potential following supra-threshold current injection was matched 1:1 by an impulse in the ventral root trace (Fig. 4Bi). Further confirmation of MN identity was provided by stimulating the ventral root in these preparations, which elicited antidromic spikes in the recorded neuron (Fig. 4Bii). The spikes occurred reliably following stimulation and at a very short latency (<2ms) confirming their antidromic nature. The identified MNs had a mean resting membrane potential of -59 +/- 5.55mV and a mean rheobase of 408.57 +/- 190.39pA following a 2ms current pulse.

Post spike afterhyperpolarisations

The output of most neural circuits changes dramatically during development to accommodate maturation of the behaviours they regulate. This is due partly to alterations in the synaptic connections between and electrical properties of the constituent neurons. With regard to the latter, post-spike hyperpolarizations are a defining feature of the responses of many neurons to excitatory inputs. In *Xenopus* tadpoles, action potentials in spinal neurons recorded at embryonic stage 37/38 are characterised by a fast (f)AHP after which the membrane potential typically returns to rest within a few milliseconds (Sautois et al. 2007). A fAHP persists at pro-metamorphic stages and was found in all recorded neurons (Fig. 5Ai). In addition, a subset of neurons at pro-metamorphic stages (15/104; 14%) displayed a pronounced slow (s)AHP following an action potential evoked from rest, which typically lasted 150-200ms (Fig. 5Ai; mean 161.29 +/- 59.99ms (n = 15)). This sAHP resembled similar responses documented in other species, which are mediated by apamin-sensitive Ca^{2+}-dependent K^{+} channels (for review see Sah and Faber 2002). However, the sAHP reported here seems to be masked during rhythmic bursting, where only fAHPs were obvious (Fig. 5Aii).

At earlier stages of *Xenopus* development (Zhang and Sillar 2012), intense firing activity in spinal neurons triggers an even longer duration AHP (approximately 60s), termed the ultra-slow (us)AHP. At pro-metamorphic stages a usAHP was evident in response to the injection of supra-threshold current pulses (Fig. 5Bi) and also following the termination of episodes of rhythmic swimming (Fig. 5Bii). Using the same stimulus paradigm as Zhang and Sillar (2012) – a train of increasing supra-threshold current pulses (Fig. 6Ai) – a direct comparison of the responses of spinal neurons at stages 37/38-42 with those at stages 50-58 was possible. The usAHP was detectable in a far higher percentage of recorded neurons (81/93(87%), including 8/9 (89%) identified MNs) at pro-metamorphic stages (50-58) as compared with stages 37/38-42 (87/202 (43%), including 39/67 (58%) identified MNs; Fig. 6Aii and see Zhang and Sillar 2012). The amplitude of the usAHP, measured as the change in membrane potential between rest and the peak slow hyperpolarisation following current injection, was similar between the two stages of development. On average, a hyperpolarisation of 4.84 +/- 2.64mV occurred at stages 37/38-42 (N=20; Zhang and Sillar 2012) while during pro-metamorphosis the hyperpolarisation was 4.66 +/- 2.6mV (N=25; ns; Fig. 6Aii). The duration of the usAHP, measured as the time between the end of the stimulus train and the point where the membrane potential returned to rest, was significantly shorter at pro-metamorphic stages. On average, the usAHP duration measured 19.33 +/- 24.50s in neurons from pro-metamorphic stages (N=25; stages 50-58), while at embryonic and early larval stages the usAHP duration was 50.78 +/- 34.21s (N=20; p<0.01; Fig. 6Aii and see Zhang and Sillar 2012).

The usAHP described in stage 37/38-42 tadpole spinal neurons is thought to be mediated solely via an increase in the activity of the Na^+ / K^+ pump and, as such, the membrane hyperpolarisation is not associated with a detectable change in membrane input resistance (IR; Zhang and Sillar 2012). During pro-metamorphosis the IR of spinal neurons was reduced, but only during the first few seconds of a usAHP (Fig. 6B). At 500ms and 2000ms after the end of the stimulus the IR was reduced significantly to 89.45 +/- 8.61 and 94.30 +/- 7.35% of control, respectively (N=9; Fig. 6Bii). The change in IR cannot account for the complete recovery of the membrane potential to rest, however, since it returned to control levels (100%) in just 6.67 +/- 7.35s, which was significantly shorter than the duration of the usAHP to the same stimulus that measured 18.58 +/- 15.33s (N=9; p<0.05, t-test; Fig. 6Biii). This suggests the usAHP comprises both a long duration Na^+ pump-based event lasting the duration of the usAHP and a superimposed event, likely caused by the opening of a membrane ion channel that is active in the early stages of the usAHP.

One candidate current to mediate such a response is the hyperpolarisation activated, Ih current. Although not reported in embryonic spinal neurons (stage 37/38), there is evidence that Ih currents emerge by larval stage 42 (Picton (2017) and pro-metamorphic *Xenopus* spinal neurons show strong evidence of possessing Ih channels (Fig. 6C). In 42/104 (40%) neurons recorded in the present study, hyperpolarization of the membrane potential caused a characteristic depolarizing sag potential, while termination of hyperpolarising pulses caused a depolarizing overshoot of the membrane potential (Fig. 6Ci). On some occasions, this post-inhibitory rebound was large enough to cause firing in the neuron (Fig. 6Cii). Ih has not previously been reported in *Xenopus* embryo spinal neurons and is thus another example of a change in the cellular properties that occur during larval development.

Based on evidence from earlier stages of *Xenopus* development (Zhang and Sillar 2012; Zhang et al. 2015), we predicted that neurons will be less likely to fire if excited within the period when the usAHP is active. To test this hypothesis the relative excitability of neurons prior to and immediately after the onset of the usAHP was investigated. Neurons with a detectable usAHP showed a reduction in excitability during the membrane hyperpolarisation (Fig. 6D). The latency to first spike following supra-threshold current injection significantly increased by 35% from 13.87 +/- 7.55ms at rest to 17.70 +/- 8.58ms, during the trough of the hyperpolarisation (Fig. 6Diii; N=17; p<0.01). Furthermore, the instantaneous spike frequency of a second spike to the current pulse was significantly reduced to 96% of that in control; 126.17 +/- 47.42Hz at rest to 121.73 +/- 48.88Hz during the usAHP (Fig. 6Diii; N=6; p<0.05). In many cases, this led to the same stimulus eliciting less spikes during the usAHP than before (Fig. 6Dii).

Modulation by nitric oxide

The behavioural repertoire expressed by an individual depends upon its developmental, ecological and arousal states at any given moment in time and neuromodulation plays an important, determinant role in sculpting behaviour to prevailing conditions. NO is known to be a potent inhibitory modulator of locomotion in embryonic and early larval stages of *Xenopus* development where it has been shown to enhance both GABAergic and glycinergic inhibition within the spinal cord (McLean and Sillar 2002, 2004). In contrast, at later pro-metamorphic stages, the effects of NO on the occurrence of spontaneous locomotor activity are excitatory (Currie et al., 2016). Moreover, the excitatory effects are thought to be mediated primarily via the brainstem in these older animals. Together these findings highlight the need to investigate the effects, if any, of NO on spinal neurons during fictive locomotion in pro-metamorphic tadpoles.

As well as increasing the occurrence of spontaneous locomotor activity (Currie et al., 2016), bath application of the NO donors SNAP (200μM; N=4) and DEA-NO (50-200μM; N=7) caused a depolarisation of spinal neurons (Fig. 7Ai, Bi). The membrane potential depolarised significantly by 8.34 +/- 7.99% relative to control during NO donor application and subsequently reduced to 6.88 +/- 7.56% of control upon washout (Fig. 7Bi; N=11, p<0.01). On average, the depolarisation was 4.03 +/- 3.21mV relative to control. The same drug application caused a reversible decrease in IR to 94.76 +/- 7.50% of control (Fig. 7Bii; N=9; 5 in DEA-NO & 4 in SNAP, p<0.05), and upon washout, the IR returned to control levels to 99.16 +/- 7.23%.

During quiescent periods, frequent depolarising postsynaptic potentials (PSPs) were observed and NO donors were found to significantly increase their frequency (Fig. 8A, Ci). The mean frequency of PSPs increased from 1.40 +/- 0.85Hz in control to 2.66 +/- 1.68Hz during NO donor application (Fig. 8Ci; N=10, 4 in SNAP and 6 in DEA-NO; p<0.05). During washout, the PSP frequency returned towards control levels to 1.43 +/- 0.85Hz. The cumulative probability of PSP inter-event interval shifted to the left, indicating a significant increase, in 5/10 recorded neurons (see example in Fig. 8Bi; p<0.05). The mean amplitude of PSPs was not significantly altered during NO donor application (Fig. 8A, Cii), however, the cumulative probability of PSP amplitude shifted to the right in 5/10 recorded neurons, indicating that the proportion of large amplitude PSPs was increased significantly compared with control in these cases (Fig. 8Bii; p<0.05).

As well as these more general effects, bath application of DEA-NO (50-200μM) also specifically reduced or, in some neurons, completely abolished the usAHP following depolarising current injection (Fig. 9A). Overall, the usAHP amplitude reduced significantly to 33.21 +/- 13.40% of the value in control; on average the amplitude was -3.42 +/- 1.54mV in control and -1.04 +/- 0.42mV during DEA-NO application (Fig. 9Ai, ii, iv; N=6, $p<0.01$). Upon washout, the usAHP amplitude recovered partially to -1.25 +/- 0.24mV or 43.08 +/- 20.13% of control (Fig. 9Aiii-iv). The effects of DEA-NO on the usAHP appear to be independent of the depolarisation during NO donor application since these effects were evident when the membrane potential was the same or even hyperpolarised vs control (e.g. Fig. 9Aii). This result is particularly interesting since it suggests that the Na^+/K^+-pump is modulable in *Xenopus* spinal neurons and therefore must be considered when investigating the neuromodulation of spinal CPG networks.

DISCUSSION

Cellular correlates of spontaneous swimming activity

We have described a new preparation that enables patch clamp recordings from spinal neurons of pro-metamorphic tadpoles during spontaneous bouts of fictive swimming. In contrast to earlier stages of development, rhythmically active neurons display a range of firing patterns during swimming activity and in response to depolarizing current pulses. One firing pattern seen in a proportion of neurons that may relate to recruitment and de-recruitment during swimming is illustrated in figure 1C. These neurons fired tonically when the ventral root was discharging low amplitude tonic activity, and then switched into a rhythmic firing pattern when the ventral root was bursting. 3/12 neurons displaying this activity pattern were identified morphologically as MNs (see Fig. 4) and therefore this pattern of firing may underlie the low-amplitude tonic activity recorded in ventral root recordings. Moreover, this pattern of activity would be suitable to provide a basal tone of muscle activation just prior to rhythmic contraction during locomotion. A bilateral stiffening of the muscles immediately rostral to those engaged in propulsive locomotion could be important to generate thrust, without causing unwanted lateral movement of the more rostral regions of the body. Other common features of these neurons were a short period of tonic ventral root discharge and neuronal firing following the end of an episode of rhythmic activity (Fig. 1Ci) or activity diminishing gradually with sporadic spiking activity (Fig.1Cii). This suggests a switch from the relatively abrupt termination of episodes in earlier stage of *Xenopus* development, often coincident with a barrage of GABAergic potentials (Reith and Sillar 1999). The ability to fire in a graded fashion may be a general feature of more mature locomotor networks. In the embryonic tadpole, neurons have two basic states: quiescent and rhythmically active. This may be sufficient for a lifestyle in which movement is solely a means of escape but would be of little use to an animal that needs to move constantly and dynamically, as in free-swimming *Xenopus* larvae. Instead, the larvae require a greater ability to change the direction and speed of locomotion as well as to selectively recruit different parts of the tail. At the cellular level, this flexibility must necessarily involve differential activation of neurons but might also involve different firing patterns such as those described here. Understanding how the firing patterns of neurons in the spinal network map onto an episode of spontaneous swimming will be an important future step in understanding how such a well-coordinated behaviour is controlled.

Another novel finding in pro-metamorphic tadpoles is that a proportion of spinal neurons fire tonically from rest (Fig. 2). No such neurons have been reported at earlier stages (37/38-42) of development. The spiking of this type of neuron is modulated during spontaneous motor activity (Fig.2A), and can switch between periods of tonic activity and rhythmic bursting (Fig. 2B). These neurons appear to represent a sub-population of spinal neurons that are continuously active, which is presumably as a result of a different set of intrinsic properties compared with other more typical CPG neurons. If a proportion of MNs were tonically active, this type of activity may contribute to a resting tone in the axial muscle of these animals that is maintained in parts of the tail that are not contributing to on-going locomotion. This type of postural control may be important in *Xenopus* swimming to facilitate their stereotypical 'hovering' during feeding, especially since there will be reduced trimming forces due to the lack of significant forward propulsion during this behaviour (Hoff and Wassersug 1986; Webb 2002). However, the fact that ventral roots are not continually active (i.e. there is no evidence for continuous low amplitude activity) may be an argument against these neurons being MNs. These tonically active neurons appear to represent a newly reported phenotype of ventral spinal neuron in *Xenopus* tadpoles that may be integral components of the neural circuitry required to generate spontaneous motor output. However, it cannot be completely ruled out that removing the dorsal half of the spinal cord during the dissection could contribute to this firing profile.

A small subset of neurons (2/104) in the pro-metamorphic spinal cord displayed intrinsic bursting in response to depolarising current injection (Fig. 3B). The membrane oscillations underlying these bursts were slow relative to fictive swim frequency, in the order of 0.5-1Hz. This is in contrast to zebrafish, where a subset of low threshold MNs display very similar, but much faster intrinsic bursting to depolarising current injection, which is thought to contribute to their propensity to be recruited at the lowest swimming speeds (Gabriel et al. 2011; Menelaou and McLean 2012). In the lamprey (Wallén and Grillner 1987) and neonatal rat (Hochman et al. 1994), similar but conditional bi-stability of the membrane potential is expressed in the presence of NMDA. Despite their relatively slow cycle period, the oscillations are proposed to contribute to the rising phase of locomotor cycles in the lamprey, since their frequency is modulated by current injection, mimicking the effects of intrinsic membrane currents during locomotion (Wallén and Grillner 1987). In early larval stages of *Xenopus,* a similar slow oscillation of spinal neuron membrane potential is found to be dependent on both NMDA and 5-HT (Scrymgeour-Wedderburn et al. 1997) and mediates a slow modulation of swimming activity over several consecutive cycles (Sillar and Reith 1998). As in the lamprey and zebrafish, the intrinsically bursting neurons described here could contribute to the fast oscillations of the membrane potential during swimming, reducing the reliance on fast synaptic inhibition for burst termination, as is the case in earlier stages of *Xenopus* development (Soffe et al. 1984; Dale 1985; Soffe 1987). Another possibility is that the intrinsic oscillations may contribute to a slower modulation of swimming that alters the intensity of motor output, and in these animals could be involved in the 'waxing and waning' of activity along the rostro-caudal axis of the body. This would be analogous to the NMDA-dependent modulation seen at earlier stages of development, controlling the relative intensity of motor bursts over the course of multiple cycles (Sillar and Reith 1998).

<u>The development of the AHPs and their role in spontaneous network activity</u>

In addition to fAHPs, which are found at early embryonic stages of development (Sautois et al. 2007), 14% of recorded pro-metamorphic spinal neurons display a pronounced slow sAHP, which typically lasts 150-200ms (Fig. 5Ai). A very similar sAHP, primarily mediated by apamin-sensitive Ca^{2+}-dependent K^+ channels is found in spinal neurons within the lamprey (Wallen et al. 1989; Hill et al. 1992; el Manira et al. 1994). This additional property of pro-metamorphic spinal neurons may offer additional opportunities for neuromodulation since the sAHP is a target for, for example, 5-HT in lamprey spinal neurons (for reviews see Grillner et al. 2001) and acetylcholine in mammalian MNs (Miles et al. 2007).

Nearly half of recorded spinal neurons (43%) at embryonic and early larval stages of *Xenopus* development display a usAHP that is dependent on increased Na^+ / K^+-pump activity following intense periods of activity (Zhang and Sillar 2012). A similar phenomenon has also been described in MNs regulating crawling behaviour in *Drosophila* larvae (Pulver and Griffith 2010) and spinal CPG neurons in mammalian locomotor networks (Picton et al. 2017). The usAHP is proposed to act as a simple mechanism for short-term memory of cellular activity that dynamically sets the excitability of neurons based on previous activity and that regulates the duration of locomotor bouts in light of previous network output. As we show here, the basic phenomenon of the usAHP persists into later, pro-metamorphic stages of *Xenopus* development (Fig. 5B, 6). However, there are several key differences. Although we cannot be sure we are comparing like with like in terms of cell type, since the majority of neurons recorded in the present study were not identified anatomically, the usAHP occurs in a far higher proportion of rhythmically active spinal neurons (Fig. 6Aii; 87% as compared with 43%). In MNs, the one cell type reliably identified in the present study, the usAHP occurred in 89% of recordings, compared to only 58% of MNs at stages 37/38-42 (Zhang and Sillar 2012), suggesting they are representative of the overall trend. Possible explanations for this more widespread expression of the usAHP are the differential expression of Na^+ / K^+-pump subunits (Azarias et al. 2013) or their accessory proteins (Cornelius and Mahmmoud 2003), or that Na^+ / K^+-pump activity is regulated via second messenger pathways (reviewed in Therien and Blostein 2000) and influenced by one of the many neuromodulators known to act on the *Xenopus* spinal CPG (Sillar et al. 2014). NO donors, for instance, were found to reduce the usAHP in these older animals (Fig. 9) and this may contribute to the overall excitatory effect of NO at these stages of development (Fig. 7, 8 and see Currie et al. 2016). At earlier stages of development, NO has net inhibitory effects on *Xenopus* locomotion (McLean and Sillar 2002, 2004) and this may be partially due to fewer network neurons being susceptible to NO's inhibitory effects on the usAHP (Zhang, Picton & Sillar, unpublished observation). A role for NO modulating the Na^+ / K^+-pump has been suggested in the rat midbrain, where it was shown to enhance NMDA-induced oscillations, mimicking the effects of increasing pump activity (Johnson et al. 1992; Cox and Johnson 1998). In the vasculature, NO donors have been shown to activate the pump (Gupta et al. 1996), however, these results are confounded by reports in both the kidney (Meffert et al. 1994) and cerebral cortex (Sato et al. 1995) where NO donors have been shown to inhibit pump activity. In fact, there is evidence that NO-mediated cell death may be partly via S-nitrosation of the sodium pump, which is one of many metabolic membrane proteins targeted by NO (Jaffrey et al. 2001).

As well as occurring in a higher percentage of recorded neurons in free-swimming *Xenopus* larvae, the usAHP is also shorter in duration (Fig. 6Aii) and associated with an initial reduction in IR (Fig. 6B) during pro-metamorphosis. The reduction in IR is only associated with the first few seconds of the usAHP and recovers significantly earlier (approximately 5s) than the duration of the usAHP (approximately 20s; Fig. 6B). Since the change in input resistance is almost certainly associated with the opening of an ion channel, and the usAHP causes a hyperpolarisation, one plausible candidate is Ih. We found evidence for the development of Ih in pro-metamorphic *Xenopus* spinal neurons, since 42/104 (40%) displayed a prominent sag response and PIR following membrane hyperpolarisation (Fig. 6C). It is possible that the usAHP interacts with Ih, which is now prevalent in spinal neurons, speeding up the recovery of the membrane potential. A similar interaction has recently been reported in leech CPG neurons (Kueh et al, 2016). Another possible explanation for the reduction in IR during the initial part of the usAHP is the opening of *Shal*-type I_A channels. Like Ih channels, these are also activated by hyperpolarisation and have been suggested to contribute to the usAHP-like responses in *Drosophila* larvae (Pulver and Griffith 2010).

<u>Nitrergic modulation of spinal neurons</u>

Given NO's excitatory effect on the occurrence of spontaneous locomotor activity during pro-metamorphosis (Currie et al. 2016), it is perhaps not surprising that NO donors were found to depolarise spinal neurons (Fig. 7) and increase PSP frequency (Fig. 8). However, evidence published previously strongly suggests that NO mediates its excitatory effects on spontaneous activity via the brainstem, and has little effect directly on the spinal network itself (Currie et al. 2016). Furthermore, at embryonic and early larval stages, NO also depolarises spinal neurons despite having a potent inhibitory effect on motor output (McLean and Sillar 2002, 2004). One possible explanation to reconcile these apparent anomalies is that pre-synaptic facilitation of depolarizing PSPs reflects the potentiation of input synapses coming from brainstem neurons involved in the descending activation of the swim CPG.

The increase in PSPs after NO donor application is not surprising given that NO is known to facilitate synaptic transmission in neurons throughout the nervous system (for review see Garthwaite and Boulton 1995). More specifically, in earlier stages of *Xenopus* development, NO is known to increase both GABAergic IPSPs onto MNs, prematurely terminating swim episodes, and NA release onto glycinergic neurons, slowing swim frequency (McLean and Sillar 2002, 2004; Fig. 2.4). NO's highly diffusible nature allows it to act on multiple neurons and synapses simultaneously, and as such any increase in NO concentration would be expected to facilitate local synaptic transmission. An important next step in these experiments is to deduce the origin of the PSPs.

In summary, we describe a novel preparation that enables patch clamp recordings from spinal neurons at later stages in the development of a well-characterised motor control system for swimming in the *Xenopus* tadpole. This preparation will now make it feasible to investigate in detail the maturation of a spinal CPG that first appeared during embryonic development and to explore the role of attendant modulatory pathways following the switch to a free-swimming life style, as well as how the new circuitry controlling the limbs becomes incorporated.

ACKNOWLEDGEMENTS

Current address for SPC is Centre for Integrative Physiology, University of Edinburgh, Edinburgh, EH8 9XD.

GRANTS

This work was supported by a PhD scholarship from the BBSRC (SPC).

DISCLOSURES

The authors declare no competing interests

REFERENCES

Azarias G, **Kruusmägi M**, **Connor S**, **Akkuratov EE**, **Liu X-L**, **Lyons D**, **Brismar H**, **Broberger C**, **Aperia A**. A specific and essential role for Na,K-ATPase α3 in neurons co-expressing α1 and α3. *J Biol Chem* 288: 2734–43, 2013.

Combes D, **Merrywest SD**, **Simmers J**, **Sillar KT**. Developmental segregation of spinal networks driving axial- and hindlimb-based locomotion in metamorphosing *Xenopus laevis*. *J Physiol* 559: 17–24, 2004.

Cornelius F, **Mahmmoud YA**. Functional modulation of the sodium pump: the regulatory proteins “Fixit”. *News Physiol Sci* 18: 119–124, 2003.

Cox BA, **Johnson SW**. Nitric oxide facilitates N-methyl-D-aspartate-induced burst firing in dopamine neurons from rat midbrain slices. *Neurosci Lett* 255: 131–4, 1998.

Currie SP, **Combes D**, **Scott NW**, **Simmers J**, **Sillar KT**. A behaviorally related developmental switch in nitrergic modulation of locomotor rhythmogenesis in larval Xenopus tadpoles. *J Neurophysiol* 115: 1446–1457, 2016.

Dale N. Reciprocal inhibitory interneurones in the Xenopus embryo spinal cord. *J Physiol* 363: 61–70, 1985.

Gabriel JP, **Ausborn J**, **Ampatzis K**, **Mahmood R**, **Eklöf-Ljunggren E**, **El Manira A**. Principles governing recruitment of motoneurons during swimming in zebrafish. *Nat Neurosci* 14: 93–99, 2011.

Garthwaite J, **Boulton CL**. Nitric Oxide Signaling in the Central Nervous System. *Annu Rev Physiol* 57: 683–706, 1995.

Grillner S, **Wallén P**, **Hill R**, **Cangiano L**, **El Manira A**. Ion channels of importance for the locomotor pattern generation in the lamprey brainstem-spinal cord. *J Physiol* 533: 23–30, 2001.

Gupta S, **Phipps K**, **Ruderman NB**. Differential stimulation of Na+ pump activity by insulin and nitric oxide in rabbit aorta. *Am J Physiol - Hear Circ Physiol* 270: H1287 LP-H1293, 1996.

Hill R, **Matsushima T**, **Schotland J**, **Grillner S**. Apamin blocks the slow AHP in lamprey and delays termination of locomotor bursts. *Neuroreport* 3, 1992.

Hochman S, **Jordan LM**, **Schmidt BJ**. TTX-resistant NMDA receptor-mediated voltage oscillations in mammalian lumbar motoneurons.. *J Neurophysiol* 72: 2559–2562, 1994.

Hoff K, **Wassersug R**. The kinematics of swimming in larvae of the clawed frog, Xenopus laevis. *J Exp Biol* 122: 1–12, 1986.

Jaffrey SR, **Erdjument-Bromage H**, **Ferris CD**, **Tempst P**, **Snyder SH**. Protein S-nitrosylation: a physiological signal for neuronal nitric oxide. *Nat Cell Biol* 3: 193–7, 2001.

Johnson SW, **Seutin V**, **North RA**. Burst firing in dopamine neurons induced by N-methyl-D-aspartate: role of electrogenic sodium pump. *Science* 258: 665–667, 1992.

Kueh D, Barnett WH, Cymbalyuk GS, Calabrese RL. Na/K pump interacts with the *h*-current to control bursting activity in central pattern generator neurons of leeches. *eLife* 5: e19322, 2016.

Li W-C, **Soffe SR**, **Roberts A**. Glutamate and acetylcholine corelease at developing synapses. *Proc Natl Acad Sci U S A* 101: 15488–93, 2004.

Li W-C, **Soffe SR**, **Wolf E**, **Roberts A**. Persistent responses to brief stimuli: feedback excitation among brainstem neurons. *J Neurosci* 26: 4026–35, 2006.

el Manira A, **Tegner J**, **Grillner S**. Calcium-dependent potassium channels play a critical role for burst termination in the locomotor network in lamprey. *J Neurophysiol* 72: 1852 LP-1861, 1994.

McLean DL, **Sillar KT**. Nitric oxide selectively tunes inhibitory synapses to modulate vertebrate locomotion. *J Neurosci* 22: 4175–84, 2002.

McLean DL, **Sillar KT**. Metamodulation of a spinal locomotor network by nitric oxide. *J Neurosci* 24: 9561–71, 2004.

Meffert MK, **Premack BA**, **Schulman H**. Nitric oxide stimulates Ca2+-independent synaptic vesicle release. *Neuron* 12: 1235–1244, 1994.

Menelaou E, **McLean DL**. A gradient in endogenous rhythmicity and oscillatory drive matches recruitment order in an axial motor pool. *J Neurosci* 32: 10925–39, 2012.

Miles GB, **Hartley R**, **Todd AJ**, **Brownstone RM**. Spinal cholinergic interneurons regulate the excitability of motoneurons during locomotion. *Proc Natl Acad Sci U S A* 104: 2448–53, 2007.

Nieuwkoop PD, **Faber J**. *Normal Table of Xenopus laevis (Daudin).* Amsterdam: North Holland Publishing, 1956.

Picton LD. The roles of dopamine and the sodium pump in the spinal control of locomotion. *University of St Andrews*. 2017.

Picton LD, **Nascimento F**, **Broadhead MJ**, **Sillar KT**, **Miles GB**. Sodium pumps mediate activity-dependent changes in mammalian motor networks. *J. Neurosci.* 37 (4): 906-921, 2017.

Pulver SR, **Griffith LC**. Spike integration and cellular memory in a rhythmic network from Na+/K+ pump current dynamics. *Nat Neurosci* 13: 53–59, 2010.

Ramanathan S, **Combes D**, **Molinari M**, **Simmers J**, **Sillar KT**. Developmental and regional expression of

NADPH-diaphorase/nitric oxide synthase in spinal cord neurons correlates with the emergence of limb motor networks in metamorphosing Xenopus laevis. *Eur J Neurosci* 24: 1907–22, 2006.

Reith CA, **Sillar KT**. Development and role of GABA(A) receptor-mediated synaptic potentials during swimming in postembryonic Xenopus laevis tadpoles. *J Neurophysiol* 82: 3175–87, 1999.

Roberts A, **Li W-C**, **Soffe SR**. How neurons generate behavior in a hatchling amphibian tadpole: an outline. *Front Behav Neurosci* 4: 16, 2010.

Sah P, **Faber ESL**. Channels underlying neuronal calcium-activated potassium currents. *Prog. Neurobiol.* 66: 345–353, 2002.

Sato T, **Kamata Y**, **Irifune M**, **Nishikawa T**. Inhibition of purified (Na+,K+)-ATPase activity from porcine cerebral cortex by NO generating drugs. *Brain Res* 704: 117–120, 1995.

Sautois B, **Soffe SR**, **Li W-C**, **Roberts A**. Role of type-specific neuron properties in a spinal cord motor network. *J Comput Neurosci* 23: 59–77, 2007.

Scrymgeour-Wedderburn JF, **Reith CA**, **Sillar KT**. Voltage oscillations in Xenopus spinal cord neurons: Developmental onset and dependence on co-activation of NMDA and 5HT receptors. *Eur J Neurosci* 9: 1473–1482, 1997.

Sillar KT, **Combes D**, **Simmers J**. Neuromodulation in developing motor microcircuits. *Curr. Opin. Neurobiol.* 29: 73–81, 2014.

Sillar KT, **Reith CA**. A role for slow NMDA receptor-mediated, intrinsic neuronal oscillations in the control of fast fictive swimming in Xenopus laevis larvae. *Eur J Neurosci* 10: 1329–1340, 1998.

Sillar KT, **Wedderburn JF**, **Simmers a J**. The development of swimming rhythmicity in post-embryonic Xenopus laevis. *Proc Biol Sci* 246: 147–153, 1991.

Sillar KT, **Wedderburn JF**, **Simmers J**. Modulation of swimming rhythmicity by 5-hydroxytryptamine during post-embryonic development in Xenopus laevis. *Proc Biol Sci* 250: 107–14, 1992.

Soffe SR. Ionic and pharmacological properties of reciprocal inhibition in Xenopus embryo motoneurones. *J Physiol* 382: 463–473, 1987.

Soffe SR, **Clarke JD**, **Roberts, A**. Activity of commissural interneurons in spinal cord of Xenopus embryos. *J Neurophysiol* 51: 1257–1267, 1984.

Therien AG, **Blostein R**. Mechanisms of sodium pump regulation. *Am J Physiol Cell Physiol* 279: C541-66, 2000.

Wallen P, **Buchanan JT**, **Grillner S**, **Hill RH**, **Christenson J**, **Hokfelt T**. Effects of 5-hydroxytryptamine on the afterhyperpolarization, spike frequency regulation, and oscillatory membrane properties in lamprey spinal cord neurons. *J Neurophysiol* 61: 759 LP-768, 1989.

Wallén P, **Grillner S**. N-Methy-D-Aspartate Receptor-induced, inherent oscillatory activity in Neurons Active During Fictive Locomotion in the Lamprey. *J Neurosci* 7: 2745–2755, 1987.

Webb PW. Control of posture, depth, and swimming trajectories of fishes. *Integr Comp Biol* 42: 94–101, 2002.

Zhang H-Y, **Issberner J**, **Sillar KT**. Development of a spinal locomotor rheostat. *Proc Natl Acad Sci U S A* 108: 11674–9, 2011.

Zhang H-Y, **Li W-C**, **Heitler WJ**, **Sillar KT**. Electrical coupling synchronises spinal motoneuron activity during swimming in hatchling Xenopus tadpoles. *J Physiol* 587: 4455–4466, 2009.

Zhang H-Y, **Picton L**, **Li W-C**, **Sillar KT**. Mechanisms underlying the activity-dependent regulation of locomotor network performance by the Na+ pump. *Sci Rep* 5: 16188, 2015.

Zhang H-Y, **Sillar KT**. Short-term memory of motor network performance via activity-dependent potentiation of Na+/K+ pump function. *Curr Biol* 22: 526–31, 2012.

FIGURE LEGENDS

Figure 1 - Whole cell patch clamp recordings during fictive locomotor activity. A: cartoon of a stage 54/55 pro-metamorphic *Xenopus laevis* tadpole. Drawing kindly provided by Laurence D. Picton, with permission. Approximate location of patch clamp recordings is indicated. B: schematic of isolated brainstem-spinal cord preparation for whole cell recording. The expanded section illustrates the site of recording with overlying dorsal spinal cord removed. Ci: both whole cell patch clamp and ventral root recordings of a spontaneous episode of fictive locomotion from a stage 55 tadpole. The lower panel shows the firing pattern on an expanded time scale to highlight the transitions between tonic and rhythmic firing during the episode. Cii: As above but for an episode evoked by brief electrical stimulation of the optic tectum. Right hand panel shows the waxing and waning of activity during the episode, including the recruitment and de-recruitment of the spinal neuron – expanded from grey box in left hand panel. * denotes stimulus artefact.

Figure 2 - Neurons with a tonic firing pattern. A: ventral root and whole cell patch clamp recordings from a stage 56 tadpole. This neuron modulates its firing rate during spontaneous episodes of motor activity (lower panels). At the beginning of the episode when the ventral root activity is highest the neuron fires at 9Hz, while just prior to the episode finishing this has dropped to only 5.5Hz.B: as above although this cell has an even more dramatic increase in firing rate at the beginning of the evoked episode of motor activity. During the episode both neuron and ventral root burst rhythmically (see lower panels).

Figure 3 - Firing properties of spinal neurons. Ai: example of typical low threshold neuron response to current injection at 1.1x and 2x rheobase. Aii: same as Ai but for higher threshold neuron. Aiii: scatter plot of current pulse vs firing frequency for the two neurons depicted in Ai (open circles) and Aii (filled circles). Bi: neuron displaying intrinsic oscillations following current injection at its firing threshold and at 2x rheobase. Bii: the same neuron during an episode of evoked swimming. Inset is part of trace within the grey box on an expanded time scale. *** denote multiple stimulation artefacts. Ci: example of a presumptive dIN firing a single spike during an episode of swimming. Cii: a spike from the same neuron evoked via current injection (black trace) with a similar evoked spike from the neuron in Fig 3Aii superimposed (grey trace). Ciii response of this neuron to current injection at its firing threshold and at 4x rheobase.

Figure 4 - Recording from motorneurons. A: neurobiotin fills of two motorneurons (MNs) from pro-metamorphic tadpoles. MNs were primarily identified based on their long descending axon (arrow in Aii,iv) that spanned several spinal segments (numbered in Ai) and exited the spinal cord via ventral root (* in Ai & iii) – soma position in Ai is marked with arrow. The arrowhead in Aiv highlights dendritic arborisations around the soma and the midline is traced with a dashed line in all panels. Unlabelled scale bars represent 50μm. Bi: ventral root and whole cell recording of a different MN following current injection in a stage 56 tadpole. Each spike in the neuron is represented 1:1 in the ventral root trace indicating the neuron projects to that root. Bii:

an antidromic spike (lower panel) from the same neuron following brief electrical stimulation of the recorded ventral root (upper panel - * denotes stimulation artefact).

Figure 5 - Afterhyperpolarisations in spinal neurons. Ai: whole cell recording at rest with 2ms suprathreshold current pulse. Following an action potential both fast (f) afterhyperpolarisation (AFP) and slow (s) AHP are visible (see insert on expanded time scale). Aii: the same neuron during motor activity highlighting the lack of any sAHPs despite the clear presence of fAHPs. Bi: whole cell recording at rest with 2s suprathreshold current pulse. Following the train of action potentials there is an ultra-slow (us) AHP lasting several seconds (see inserts for expansion of the first few seconds). Bii: the same neuron and a ventral root recording during spontaneous motor activity. Following membrane repolarisation at the termination of swimming there is an usAHP lasting several seconds (see insert for expansion of first few seconds).

Figure 6 - The development of the usAHP. Ai: whole cell recording during 10pA current steps from -50pA to 260pA (protocol was stopped after 20th suprathreshold current step). The protocol (originally used in Zhang & Sillar, 2012) drives an usAHP in the neuron and basic parameters can be measured. Aii: direct comparison of usAHP between stages 37/38-42 (N = 25; Zhang & Sillar, 2012) and pro-metamorphic stages 50-58 (N = 20). Bi: whole cell recording with hyperpolarising steps both prior to and after driving an usAHP (NB: action potentials are truncated; see expansion for details of protocol). Bii: graph of input resistance (IR) at successive hyperpolarising steps following the usAHP relative to IR at rest. Biii: graph of mean time taken for IR to return to baseline levels and mean duration of the usAHP to the same protocol (N = 9) Ci: whole cell recording showing a typical response to successive hyperpolarising steps from rest. Membrane sag and post inhibitory rebound (PIR) are highlighted. Cii: whole cell recording from the same cell showing how PIR often leads to rebound action potentials following membrane repolarisation. Di: whole cell recording during successive supratheshold current steps highlighting the loss of neuronal excitability during the usAHP (NB: action potentials are truncated). Bii: comparison of neuronal response to short suprathreshold current injection before (black trace) and after (grey trace) driving an usAHP. Diii: mean data for the same protocol showing the latency to the first spike (N = 17) and instantaneous firing frequency of the second spike (N = 6) after the usAHP relative to before it. * denotes p = < 0.05; *** denotes p = < 0.01 from a paired t-test (Aii, Biii) or a Wilcoxon signed rank test (Bii, Diii).

Figure 7 - Nirtergic modulation of pro-metamorphic spinal neurons. A: ventral root and whole cell recordings during bath application of 200μm DEA-NO. A reversible increase in resting membrane potential (RMP) is visible in the whole cell record (Ai, bottom panel). Aii: on expanded time scales examples of spontaneous episodes motor activity are shown. B: graphs of mean RMP (Bi) and input resistance (IR; Bii) relative to control during NO donor application (200μm SNAP, N = 4; 200μm DEA-NO, N = 7) and during washout. * denotes p = < 0.05; *** denotes p = < 0.01 from a Wilcoxon signed rank test.

Figure 8 - Nitric oxide increases PSPs in spinal neurons. A: a whole cell recording from 3 quiescent periods during control, DEA-NO application and washout showing depolarising post-synaptic potentials (PSPs). B: cumulative frequency plots for PSP inter-event interval (Bi) and amplitude (Bii) for the cell recorded in A. C: average data for PSP frequency (Ci) and amplitude (Cii) during control, NO donor application (200μm SNAP, N = 4; 200μm DEA-NO, N = 6) and washout. * denotes $p = < 0.05$ from a repeated measures ANOVA with Bonferroni correction .

Figure 9 - Nitric oxide blocks the usAHP in pro-metamorphic neurons. Ai-iii: whole cell recording of response to suprathreshold current steps before (Ai), during (Aii) and after (Aiii) bath application of 200μm DEA-NO (action potentials are truncated). Div: average data of usAHP amplitude relative to control during 200μm DEA-NO application and during washout (N = 6). *** denotes $p = < 0.01$ from a Wilcoxon signed rank test.

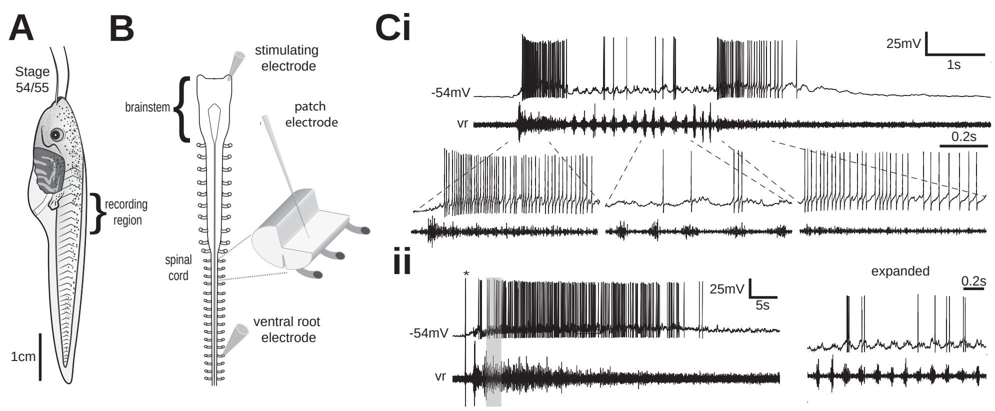

A
Stage
54/55
recording
region
1cm
B
stimulating
electrode
brainstem
patch
electrode
spinal
cord
ventral root
electrode
Ci
25mV
1s
-54mV
vr
0.2s
ii
*
25mV
5s
-54mV
vr
expanded
0.2s

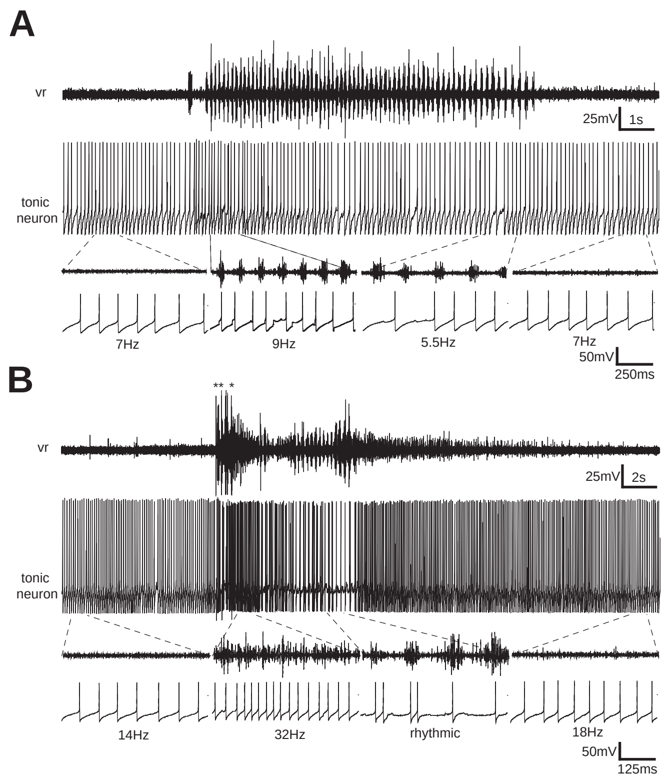
A
vr
25mV
1s
tonic
neuron
7Hz
9Hz
5.5Hz
7Hz
50mV
250ms
B
** *
vr
25mV
2s
tonic
neuron
14Hz
32Hz
rhythmic
18Hz
50mV
125ms

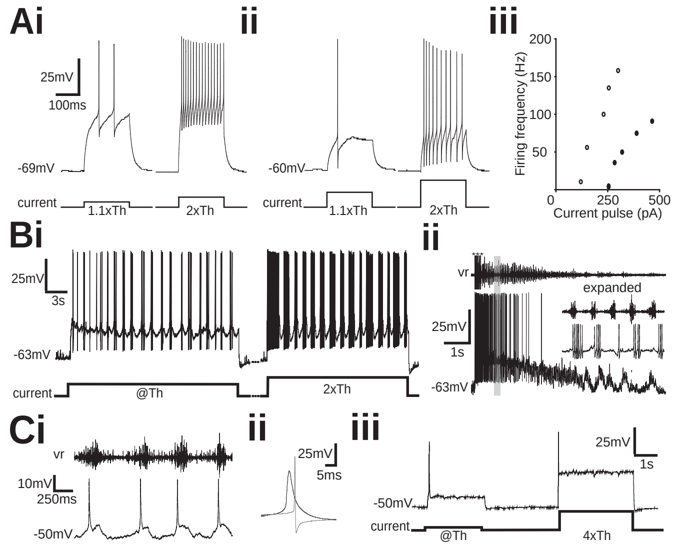
Ai
ii
iii
25mV
100ms
-69mV
-60mV
current
1.1xTh
2xTh
Firing frequency (Hz)
200
150
100
50
0
250
500
Current pulse (pA)
Bi
ii
25mV
3s
-63mV
@Th
vr
expanded
1s
Ci
vr
10mV
250ms
-50mV
5ms
4xTh

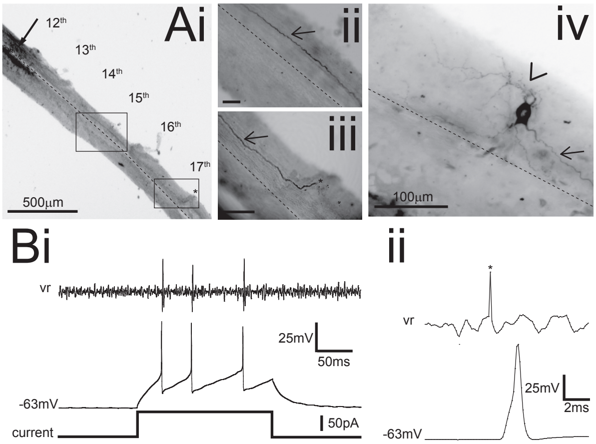
Ai
12th
13th
14th
15th
16th
17th
*
500μm
ii
iii
*
iv
100μm
Bi
vr
25mV
50ms
-63mV
current
50pA
ii
*
vr
25mV
2ms
-63mV

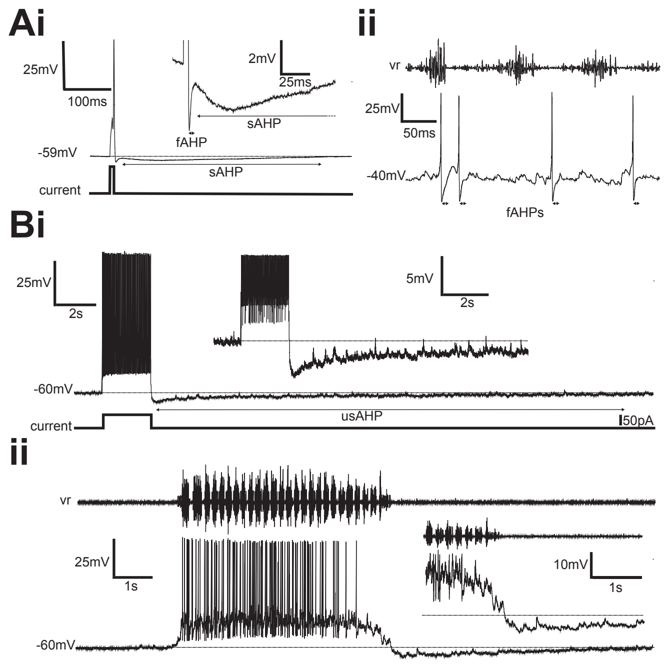

Ai
25mV
100ms
2mV
25ms
fAHP
sAHP
-59mV
sAHP
current
ii
vr
25mV
50ms
-40mV
fAHPs
Bi
25mV
2s
5mV
2s
-60mV
current
usAHP
50pA
ii
vr
25mV
1s
10mV
1s
-60mV

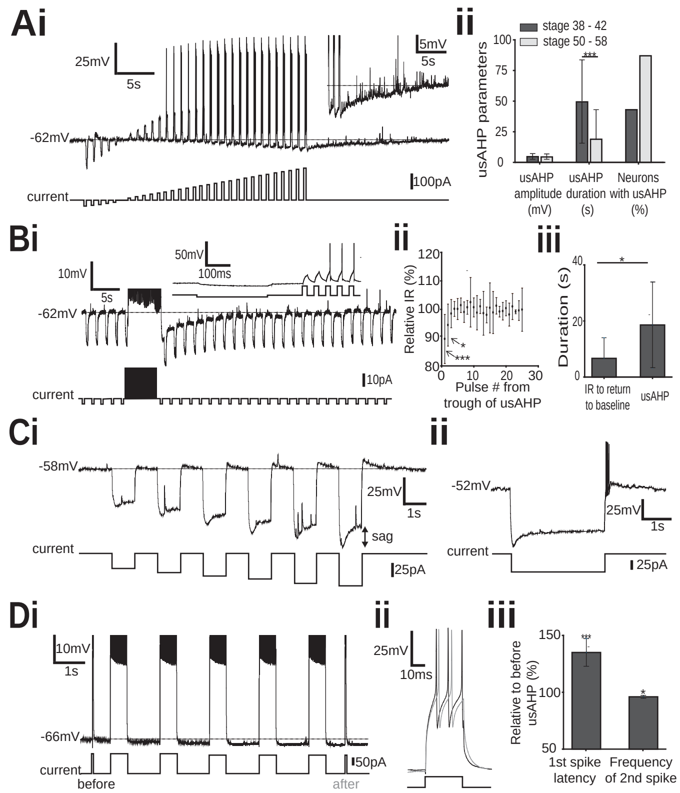

Ai
ii
25mV
5s
5mV
5s
-62mV
current
100pA
stage 38 - 42
stage 50 - 58
usAHP parameters
***
usAHP amplitude (mV)
usAHP duration (s)
Neurons with usAHP (%)
Bi
ii
iii
10mV
5s
50mV
100ms
-62mV
current
10pA
Relative IR (%)
Pulse # from trough of usAHP
Duration (s)
IR to return to baseline
usAHP
Ci
ii
-58mV
25mV
1s
sag
current
25pA
-52mV
25mV
1s
current
25pA
Di
ii
iii
10mV
1s
-66mV
current
50pA
before
after
25mV
10ms
Relative to before usAHP (%)
1st spike latency
Frequency of 2nd spike

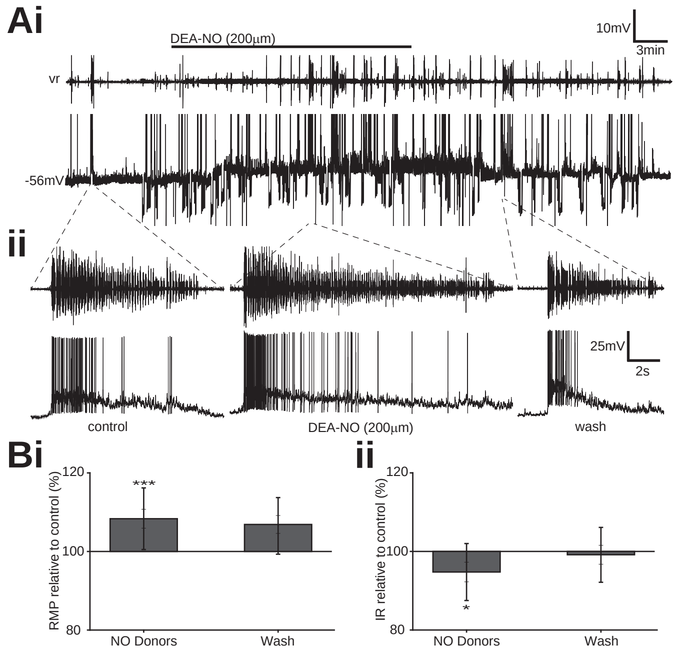
Ai
DEA-NO (200μm)
10mV
3min
vr
-56mV
ii
25mV
2s
control
DEA-NO (200μm)
wash
Bi
RMP relative to control (%)
120
100
80
***
NO Donors
Wash
ii
IR relative to control (%)
120
100
80
*
NO Donors
Wash

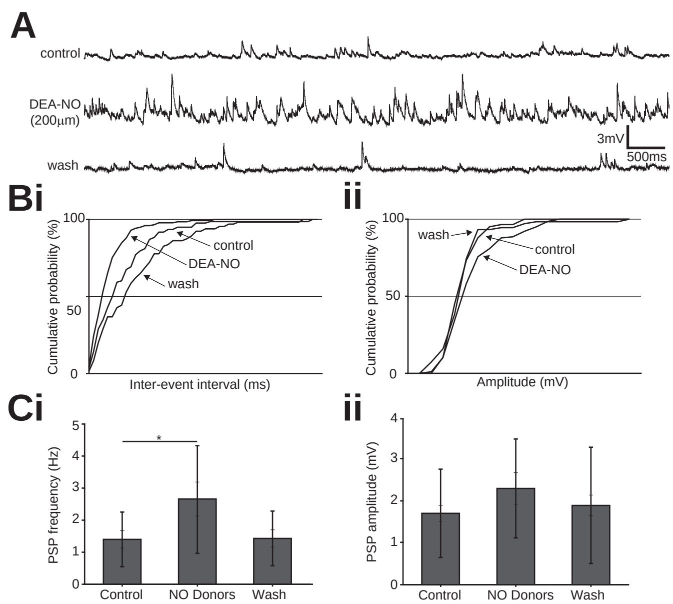
A
control
DEA-NO
(200μm)
3mV
500ms
wash
Bi
100
50
0
Cumulative probability (%)
control
DEA-NO
wash
Inter-event interval (ms)
ii
100
50
0
Cumulative probability (%)
wash
control
DEA-NO
Amplitude (mV)
Ci
PSP frequency (Hz)
5
4
3
2
1
0
*
Control
NO Donors
Wash
ii
PSP amplitude (mV)
4
3
2
1
0
Control
NO Donors
Wash

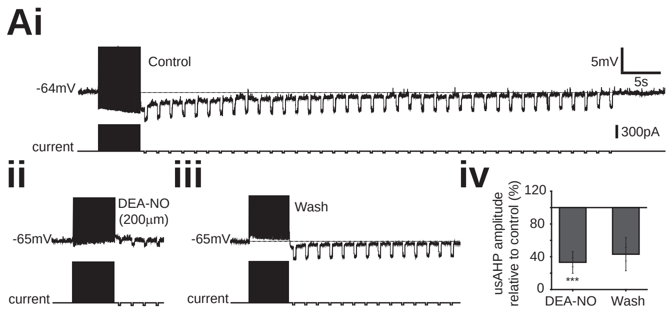

Ai
Control
-64mV
5mV
5s
current
300pA
ii
DEA-NO
(200μm)
-65mV
current
iii
Wash
-65mV
current
iv
usAHP amplitude
relative to control (%)
120
80
40
0
***
DEA-NO
Wash